ELSEVIER

Contents lists available at ScienceDirect

European Journal of Pharmacology

journal homepage: www.elsevier.com/locate/ejphar





Novel apocynin regulates TRPV1 activity in the trigeminal system and controls pain in a temporomandibular joint neurogenic model

Taisa Maria Mendes Matuiama Machado ^{a,1}, Iara Gonçalves Aquino ^{a,1}, Marcelo Franchin ^{b,c}, Miguel O. Zarraga ^d, Daniel Bustos ^{e,f}, Fernanda Papa Spada ^g, Marcelo Henrique Napimoga ^a, Juliana Trindade Clemente-Napimoga ^a, Severino Matias Alencar ^g, Bruna Benso ^{h,**}, Henrique Ballassini Abdalla ^{a,*}

- ^a Faculdade São Leopoldo Mandic, Campinas, SP, Brazil
- ^b School of Dentistry, Federal University of Alfenas (Unifal-MG), Alfenas, MG, Brazil
- ^c Bioactivity and Applications Lab, Department of Biological Sciences, Faculty of Science and Engineering, School of Natural Sciences, University of Limerick, Limerick, Ireland
- ^d Department of Organic Chemistry, Faculty of Chemical Sciences, Universidad de Concepcion, Concepcion, Chile
- e Centro de Investigación de Estudios Avanzados del Maule (CIEAM), Vicerrectoría de Investigación y Postgrado, Universidad Católica del Maule, Talca, Chile
- f Laboratorio de Bioinformática y Química Computacional (LBQC), Escuela de Bioingeniería Médica, Facultad de Medicina, Universidad Católica del Maule, Talca, Chile
- g Department of Agri-Food Industry, Food, and Nutrition, Luiz de Queiroz College of Agriculture, University of São Paulo (USP), Piracicaba, SP, Brazil
- h School of Dentistry, Faculty of Medicine, Pontificia Universidad Catolica de Chile, Santiago, Chile

ARTICLE INFO

Keywords: Apocynin Chalcone TRPV1 Orofacial pain Trigeminal ganglion Galleria mellonella

ABSTRACT

Objective: Herein, we investigate the potential analgesic effect of a newly synthesized chalcone-derived apocynin in a neurogenic pain model.

Methods: Molecular docking was used to foretell the apocynin binding features and dynamics with the TRPV1 channel, and the activity was tested in vitro, using transfected HEK 293T cells with the rat TRPV1 receptor. The analgesic effect of apocynin was investigated using a capsaicin-induced pain model. The expression of TRPV1, TRPA1, TRPM8, and MAPKs was assessed by electrophoresis, and immunosorbent assays were performed to quantify the neurotransmitters Substance P, Glutamate, and CGRP. A survival assay using Galleria mellonella was carried out to determine the toxicity.

Results: We observed that apocynin exhibits greater thermodynamic stability. Upon apocynin ligand binding, it changes the electrostatic potential for a predominantly electronegative state in the interior and neutral in its external vanilloid pocket. Treatment of apocynin induces antinociceptive effects against the noxious challenge of capsaicin. Histologically, apocynin decreased the number of TRPV1⁺ immunopositive cells. Electrophoresis showed reduced phosphorylation of p44/42 (ERK1/2) and decreased protein levels of substance P, and CGRP. In the survival assay, apocynin showed low toxicity.

Conclusions: In conclusion, we provide proof-of-principles that the newly synthesized apocynin compound effectively prevented nociception in a neurogenic model of orofacial pain.

Abbreviations: APBS, Adaptive Poisson-Boltzmann Solver; Apo, Apocynin; CAP, Capsaicin; CCOHS, Canadian Centre for Occupational Health and Safety; CGRP, Calcitonin Gene-Related Peptide; CZP, Capsazepine; DRG, Dorsal Root Ganglion; ERKs, Extracellular Signal-Regulated Kinases; IC50, Half Maximal Inhibitory Concentration; ICOP, International Classification of Orofacial Pain; JNK, c-Jun N-terminal Kinases; LD50, Median Lethal Dose; MAPK, Mitogen-Activated Protein Kinase; MDs, Molecular Dynamics Simulation; MM-GBSA, Molecular Mechanics-Generalized Born Surface Area; NPT, Number of particles, Pressure, and Temperature; NSAIDs, Nonsteroidal Anti-inflammatory Drugs; PDB, Protein Data Bank; POPC, 1-Palmitoyl-2-oleoyl-phosphatidylcholine; RGS, Rat Grimace Scale; RMSD, Root Mean Square Deviation; SPC, Single Point Charge; TG, Trigeminal Ganglion; TMJ, Temporomandibular Joint; TRPA1, Transient Receptor Potential Ankyrin 1; TRPM8, Transient Receptor Potential Melastin 8; TRPV1, Transient Receptor Potential Vanilloid 1; VMD, Visual Molecular Dynamics.

E-mail addresses: bruna.benso@uc.cl (B. Benso), henrique.abdalla@slmandic.edu.br (H.B. Abdalla).

^{*} Corresponding author. Faculdade São Leopoldo Mandic, Instituto e Centro de Pesquisas São Leopoldo Mandic, Rua José Rocha Junqueira, 13 – Swift, CEP: 13405-755, Campinas, SP, Brazil.

^{**} Corresponding author.

¹ Equally contribute to this work.

1. Introduction

According to the International Classification of Orofacial Pain (ICOP), orofacial pain is defined as "pain caused by diseases, injuries or abnormal functioning of the tooth pulp, periodontium, gingiva (e), oral mucosa, salivary glands or jaw bone tissue, or by normal functioning of the tooth pulp signalling risk of tooth damage" (ICOP, 2020). The primary sensory neurons that innervate the orofacial regions are located in the trigeminal ganglion and recognize the external stimulus, taking the nociceptive information to higher centers where pain is processed and perceived (Liu et al., 2022). Additionally, immune cells (i.e., macrophages, neutrophils, satellite glial cells, etc.) play crucial roles in nociceptive signal transmission by increasing cytokines and neuropeptides release, activating intracellular pathways, leading to a facilitation of action potential transmission (Abdalla et al., 2022a,b; Mecklenburg et al., 2023).

Particularly, neurogenic inflammation is a complex process initiated by the activation of sensory nerves, particularly trigeminal afferents, which release neuropeptides such as calcitonin gene-related peptide (CGRP) and substance P (SP). These neuropeptides play a key role in the inflammatory response by promoting vasodilation, which increases blood flow to the affected area (Biscetti et al., 2023). Additionally, the release of these neuropeptides induces mast cell degranulation, a process that further amplifies the inflammatory cascade by releasing histamine and other pro-inflammatory mediators. This combination of increased vascular permeability, immune cell activation, and the recruitment of inflammatory molecules underpins the pathophysiology of neurogenic inflammation, contributing to pain and tissue sensitivity often observed in conditions such as migraine, arthritis, and chronic pain syndromes (Kilinc et al., 2024)

Given this framework and considering the multi-complexity associated with painful states in the orofacial area (e.g., genetics, environment, behavior, medication, psychological stress, anxiety, obsessivecompulsive feelings, pain-coping strategies, and sleep quality), management of these conditions is challenging (Ettlin et al., 2021), especially regarding pharmacotherapy. Cases of acute pain episodes are usually managed with nonsteroidal anti-inflammatory drugs (NSAIDs) and other over-the-counter medications (ibuprofen, acetaminophen, corticoids), aside from additional non-pharmaceutical treatments (physical therapy, occlusal splint), and pain sensation is controlled (Harper et al., 2016; Ghurye and McMillan, 2017). On the other hand, chronic pain like trigeminal neuropathies is demanding. Antidepressants, anticonvulsants, and opioids are commonly prescribed with low rates of effectiveness. In addition, depending on how long and the dosage used, side effects may occur as neurological side effects, hyponatremia, blood disorders, weight gain, addiction, constipation, mood changes, and sexual dysfunction (Harper et al., 2016; Ghurye and McMillan, 2017).

Transient receptor potential vanilloid 1 (TRPV1), also known as capsaicin receptor, is activated by heat, voltage, and specific ligands. In peripheral nerve fibers, it serves as a thermal and chemical sensor in nociceptive paths. TRPV1 receptor is a nonselective cation channel. Activation leads to the generation of the action potential through the inflow of both Na⁺ and Ca²⁺ ions (Liang et al., 2023). In this regard, TRPV1 has been associated with pain sensation in several circumstances (e.g., neuropathic, itch, inflammatory), being considered a promising therapeutic target in the management of pain (Davis et al., 2000; Liang et al., 2023). Apocynin is a new chalcone derivate with interesting pharmacological effects and it can be isolated from many plant or chemically synthesized (Klees et al., 2006). Furthermore, chalcone is a derived-natural product with proven anti-inflammatory, antimicrobial, and antifungal properties, and serves as an inhibitor of nociception, partially justified by its modulatory effects on the TRPV1 receptor (Benso et al., 2019). Considering this, our research group has synthesized a newly chalcone derivative of apocynin, 1-(4-hydroxy-3-methoxyphenyl)-3-(4-nitrophenyl)-2- propenone (Moreno 2020;

Bustos et al., 2023).

Therefore, in the present manuscript, we explore the potential analgesic effects of the new apocynin compound using a neurogenic model induced by capsaicin. We investigate their capacity to counteract the TRPV1 receptor in the trigeminal ganglion and inhibit neurotransmitter release. For last, we carried out a survival assay to determine toxicity.

2. Material and methods

2.1. Chemistry

The synthesis of apocynin was carried out by applying the Claisen-Smith reaction both by means of alkaline or acid catalysis. The details about the procedures of synthesis as well as spectroscopic characterization are previously described (Moreno 2020).

2.2. In vitro screening and biological evaluation

The activity of apocynin was evaluated on capsaicin and temperature-induced TRPV1 activation. Both responses were measured into transfected HEK 293T cells (ATCC CRL-3216 $^{\rm TM}$) with rat TRPV1 receptor and were determined using a high throughput calcium influx assay in which Fluo-4 AM fluorescence was followed in a real-time PCR thermocycler (Luo et al., 2011) allowing us to follow multiple conditions simultaneously during a temperature ramp.

2.3. Computational Methodology

The 3D structure of the TRPV1 channel in mammals, with the Protein Data Bank (PDB) identifier 7LR0 (Nadezhdin et al., 2021), served as the foundational structure for our study. We employed an ensemble docking approach to investigate the binding of the apocynin (Apo) ligand. To prepare the protein structure and its co-crystallized ligand capsaicin (CAP), we utilized the Maestro/Schrödinger software suite (Release, 2021-1 - Schrödinger, Inc. [Maestro, 2020]). Protonation states were assigned with Propka (Olsson et al., 2011) based on physiological pH conditions. Subsequently, the system underwent energy minimization, with the optimization limited to hydrogen atoms to preserve the initial structure. Next, we embedded the TRPV1-CAP complex within a lipid membrane composed of 1-Palmitoyl-2-oleoyl-phosphatidylcholine (POPC). Additionally, the system was solvated within a periodic box containing Single Point Charge (SPC) water molecules, and an ionic concentration of 150 mM NaCl was added to mimic physiological conditions. The prepared system was subjected to an extensive 0.5 µs molecular dynamics simulation (MDs) using the OPLS3e force field (Roos et al., 2019) within the Desmond simulation package of Maestro/Schrödinger suite (Maestro, 2020). The simulation was conducted under NPT (constant Number of particles, Pressure, and Temperature) conditions with a pressure (P) of 1 atm and a temperature (T) of 300 K. No energy restraints was applied during the simulation. Upon completion of the MDs, we exported 2000 frames of the protein, excluding the CAP ligand from the vanilloid binding site. Each frame represented a time interval of 0.25 ns during the simulations. These frames were utilized as input data for constructing a dendrogram based on Root Mean Square Deviation (RMSD) using the Bio3D library (Grant et al., 2021). Subsequently, we identified 10 distinct clusters within the dendrogram, each representing a conformational state explored by the protein during the simulation. These representative frames from each cluster were employed for molecular ensemble-docking of the Apo compound. To facilitate this, we generated a total of 40 grids, one for each representative frame of the cluster, and for each of the four monomers constituting the channel. Each grid was sufficiently large to encompass the reported modulation sites within the channel, including the vanilloid site and the regions above and below the selectivity filter. The Apo ligand was prepared for docking using the Maestro/Schrödinger

2D-sketcher module, followed by geometric optimization. Protonation states were assigned using the Epik module (Shelley et al., 2007) under physiological pH conditions. Docking simulations were performed utilizing the Glide program (Halgren et al., 2004) within the same molecular suite, employing the SP scoring function. For each docked Apo ligand, a maximum of 10 docking poses were generated in a single run. Subsequently, all data were exported into a data frame in the R processing language v.4.3.1 for further analysis. We then identified the conformational state in each of the four monomers of the channel that exhibited the most energetically favorable binding poses for the Apo ligand. To validate our findings and for comparative analysis, we performed a $0.5 \,\mu s$ simulation of the TRPV1-Apo complex in its four binding sites, utilizing the same simulation conditions as employed for the previously mentioned TRPV1-CAP complex. Furthermore, we conducted an analogous simulation with the inhibitory molecule capsazepine (CZP) using the crystal structure TRPV1-CZP (PDB id: 5ISO [Gao et al., 2016]). Following the completion of the three MDs, we conducted a comprehensive evaluation of the binding interactions between three ligands, namely CAP, CZP, and Apo, and the TRPV1 channel in its four binding sites. This evaluation encompassed energetic, thermodynamic, and geometric aspects.

2.3.1. Thermodynamic analysis

We initiated our analysis by examining the thermodynamic stability of both the protein and the ligands over the course of the simulations. This assessment was carried out by calculating the RMSD values.

2.3.2. Geometric analysis

Subsequently, we performed a geometric analysis of the electrostatic potential surface within the vanilloid binding site following the binding of each ligand. For this, the adaptive Poisson-Boltzmann Solver (APBS) software (Baker et al., 2001) was used to compute the surface as an average over the entire trajectory and visual molecular dynamics (VMD) for its visualization (Humphrey et al., 1996). This analysis allowed us to gain insights into the spatial distribution of electrostatic charges within the binding site and its significance in ligand binding. Additionally, we investigated the intermolecular interactions that govern the affinity of the protein-ligand complex in each case.

2.3.3. Affinity energy calculation

To quantify the binding affinity of each complex, we exported 200 frames from each simulation, representing time intervals of 2.5 ns throughout the trajectory. These frames were used to calculate the binding affinity energy of each complex using the Molecular Mechanics-Generalized Born Surface Area (MM-GBSA) method. This calculation was performed within the Prime module (Jacobson et al., 2004) of the Maestro/Schrodinger suite.

2.4. Animals

Male Wistar rats (total number of animals = 44) were bought from Anilab (Paulínia – São Paulo, Brazil) and maintained in pathogen-free conditions at $24^{\circ} \pm 0.5 \,^{\circ}$ C, with a light/dark cycle of 12:12 h, with food and water ad libitum. Animals were randomly assigned to conventional plastic cages containing aspen wood as bedding material and environmental enrichment. All experiments were approved by the Committee on Animal Research of Faculdade São Leopoldo Mandic (2022/33) and are reported in compliance with the ARRIVE guidelines (Kilkenny et al., 2010). The number of animals used was 5 per group and each animal was used once. The number of animals used was the minimum necessary to reach statistical power and based on previously published studies (Abdalla et al., 2021, 2022; Mazuqueli Pereira et al., 2021). The sample size of each experimental group is described in each figure legend.

2.5. Nociceptive assessment

The nociceptive assessment was performed during the light phase (from 8:00 a.m. to 5:00 p.m.) in a quiet room. Preliminary to any procedure, rats were kept in the test chamber for 15 min to minimize stress related to the new environment. The rats were submitted to handling protocols for 7 days before the beginning of the nociceptive analysis. The protocol consisted of holding and manipulating the animals for 3–5 min daily for a week. Also, rats were placed into the test chamber for 10 min due to the habituation process for the new environment. On the day test, rats were previously anesthetized by inhalation of isoflurane, and the intra-temporomandibular joint (TMJ) injection was performed as previously described (Abdalla et al., 2022a,b). In order to induce neurogenic pain in the temporomandibular joint (TMJ), a 1.5% capsaicin solution was intra-articular injected unilaterally, following previous publications (Pelissier et al., 2002; Rocha-Neto et al., 2019). The capsaicin solution was prepared using 10% capsaicin in a mixture of ethanol, Tween 80, and sterile saline in a 1:1:8 ratio by volume, as outlined by Lam et al. (2005). Rats were placed back to the test chamber to completely regain consciousness (30-60s after discontinuing the anesthesia), and then the nociceptive response was evaluated over 30 min. The term "response" referred to the total number of seconds the animal spent rubbing the orofacial region with the fore or hind paw and the number of head flinches observed during the study period. Each head flinch was counted as 1 s. Therefore, the sum of the two behaviors was used as a nociceptive response. (Lamana et al., 2017). The recording time was divided into 10 blocks of 3 min each. At the end of each behavior test, the rats were immediately euthanized by deep anesthetizing, and their trigeminal ganglion was removed. All the behavior analyses were conducted in a fashion where the treatments and injections given were blinded to who analyzed the behavior response.

2.6. Rat Grimace Scale (RGS)

The nociceptive behavior was recorded in a manner that permitted a complete view of each animal. Rats were continually recorded during their behavioral responses, split across three blocks of 5 min with a 4-min interval between each block $(0-5',\,9-14',\,$ and 18-23'). After that, the videos were examined by a blinder experimenter. A 0-2 score (0= not present, 1= moderate, and 2= obvious pain) was appointed to each facial parameter (orbital tightening, nose/cheek flattening, ear changes, and whisker changes) observed in each 5-min block, as earlier defined (Sotocinal et al., 2011). The mean of the scores was considered the total RGS score.

2.7. Experimental design

The experimental designs are summarized in Fig. 2A and E.

2.7.1. Effect of Apo on capsaicin challenge in TMJ

To assess whether apocynin could prevent neurogenic nociception induced by capsaicin in TMJ, groups of rats (n = 5) were pre-treated with an intra-TMJ injection of apocynin (0, 1, 10, 100, and 200 ng/15µl/TMJ). Control group received an intra-articular injection of saline solution (0,9%/30µl/TMJ). After 15 min, animals were challenged with an intra-TMJ injection of capsaicin (1.5%/30µl/TMJ). The nociceptive behavioral response was quantified over 30 min (Rocha-Neto et al., 2019). Immediately at the end of the nociceptive testing, animals were euthanized, and their trigeminal ganglion was removed and stored.

2.7.2. Evaluation of the systemic or local effect of apocynin on capsaicin challenge in TMJ

To verify whether apocynin was inducing antinociception peripherally or systemically, a group of rats (n = 5) was pre-treated with a contralateral intra-TMJ injection of Apo (200ng/15 μ l/TMJ) 15 min before the noxious challenge. Then, animals were challenged with an

ipsilateral intra-TMJ injection of capsaicin (1.5%/ 30μ l/TMJ), and the nociceptive behavioral response was quantified over 30 min.

2.8. Sample preparation for protein extraction

For trigeminal ganglion collection, the neurocranium was opened, and the entire brain was removed. The trigeminal ganglion was visualized in Meckel's cave in the dura mater close to the apex of the petrous part of the temporal bone (Rocha-Neto et al., 2019). The trigeminal ganglion was carefully removed, and the samples were stored in a $-80\,^{\circ}\text{C}$ freezer until processing. Samples were homogenized in 300 μL of RIPA lysis and extraction buffer (Santa Cruz) containing protease (Protease Inhibitor Cocktail 100X #Cell Signaling 5871S; 1:1000) and phosphatase inhibitor (Phosphatase Inhibitor Cocktail 100X #Cell Signaling 5870S; 1:1000). Samples were homogenized using a high-speed benchtop homogenizer, followed by centrifugation for 10 min at 10,000g and 4 °C and the supernatants collected and stored at $-20\,^{\circ}\text{C}$. Total protein was measured with the Micro BCA Protein Assay Kit (Thermo Scientific).

2.9. Enzyme-linked immunosorbent assay (ELISA)

Supernatants of trigeminal ganglia were used to measure protein levels of neuropeptides substance P (EIAR-SP-2; RayBiotech), calcitonin gene-related peptide (CGRP) (EIAR-CGRP-2; RayBiotech), and glutamate (MBS756400; MyBioSource) through enzyme-linked immunosorbent assay. The assays were performed according to the manufacturer's protocol.

2.10. Western blotting

Protein lysates from trigeminal ganglion samples for western blotting reactions were performed as previously described (Abdalla et al., 2022a, b). Thirty micrograms of each protein lysate were probed with primary antibodies against anti-TRPV1 (1:500; Alomone Labs), anti-transient receptor potential ankyrin 1 (TRPA1) (1:500; Alomone Labs), anti-transient receptor potential melastin 8 (TRPM8) (1:250; Alomone Labs), p38 MAPK (1:1.000; Cell Signaling), p44/42 MAPK (1:1.000; Cell Signaling), SAPK/JNK (1:1.000; Cell Signaling), Phospho-p38 MAPK (Thr180/Tyr182; 1:1.000; Cell Signaling), Phospho-p44/42 MAPK (Erk1/2; 1:1000, Cell Signaling), Phospho-SAPK/JNK (Thr183/Tyr185; 1:1000, Cell Signaling), and GAPDH (1:1.000, Cell Signaling). Protein bands were visualized using SuperSignal® West Pico Chemiluminescent Substrate (Thermo Fisher Scientific) and ImageQuantTM LAS 4000 mini gel documentation (GE Healthcare). Densitometric analysis of bands was performed with the ImageJ software (National Institutes of Health).

2.11. Immunohistochemistry

For the immunohistochemistry, another set of experiments was conducted. The trigeminal ganglion was carefully removed and fixed in 10% formaldehyde for three days. Then, trigeminal ganglions were dehydrated and paraffin-embedded and cut into 3 μm sections. After that, the sections were deparaffinized and hydrated, and three immersions of the slides quenched endogenous peroxidase activity in 3% hydrogen peroxide for 5 min each. The blocking was made with 5% nonfat dry milk for 30 min. The antigen retrieval was assembled in a steamer with citrate buffer (pH 6.0) for 20 min at 97 $^{\circ}$ C and 10 min at room temperature. The trigeminal ganglion (TG) section was then incubated overnight at 4 °C with a primary antibody for anti-TRPV1 (1:250; Alomone Labs). After primary antibodies incubation, the sections were then incubated with secondary antibody Advance HRP Detection System (Dako Corp), treated with DAB (3,30-diam-inobenzidine tetrahydrochloride Dako Corp) for 10 min and counter-stained with Mayer's Hematoxylin for 5 min at room temperature. Images were obtained using an optical microscope using a Zeiss Axioskop 2 Plus microscopy (Zeiss).

The images were taken from the mandibular branch of the trigeminal ganglion. Three blinded experimenters quantified the positive immune cells. The counting was carried out in 4 different fields of each section (n = 3 per group).

2.12. In vivo toxicity in Galleria mellonella

To determine the *in vivo* toxicity of apocynin, we carried out a survival assay on *Galleria mellonella* larvae model, as previously described with modifications (Megaw et al., 2015; Rochelle et al., 2016). The Larvae source was the Biochemistry and Instrumental Analysis Laboratory (ESALQ/USP). Larvae were grown at 28 °C, and those weighing 200–300 mg, were randomly selected (n = 15/group). Each larva received 10 μ L of apocynin in one of seven groups, with concentrations ranging from 0.1 mg/kg to 1000 mg/kg, or mineral water (control group), administered into the hemocoel via the last left proleg. All groups were incubated at 28 °C, and survival was monitored at 24 h for up to 72 h. Larvae showing high melanization and absence of movements upon touch were counted as dead (Rochelle et al., 2016).

2.13. Statistical analysis

Results were expressed as the mean \pm standard deviation (SD). Animal's findings were analyzed per one-way analysis of variance (ANOVA) and post hoc Tukey test, with significance set at P < 0.05. The percent survival of *Galleria mellonella* larvae was compared using the log-rank Mantel—Cox test. The data were analyzed in GraphPad Prism, version 10.2 for Windows (GraphPad Software)

3. Results

3.1. Standardization of apocynin features and dynamics

We assessed the thermodynamic stability of the protein through RMSD measurements. Our analysis reveals that the TRPV1-CZP and TRPV1-Apo complexes exhibit greater stability compared to TRPV1-CAP, the latter displaying a more fluctuating profile throughout the simulation. The observed differences in thermodynamic stability, as reflected in the RMSD profiles (Fig. 1A), can be attributed primarily to the dynamics of specific helices. Helices 1 and 2 display an extended conformation relative to helices 3 and 4, contributing to the observed fluctuations. Remarkably, despite these subtle movements, the position of CAP within the vanilloid site remains remarkably stable. This pattern is consistent across all three systems, as evident in the RMSD profiles of the ligands (Fig. 1B). Particularly noteworthy is the relatively higher instability observed for the apocynin ligand within the vanilloid site when compared to the other two ligands. However, it's essential to emphasize that a thorough visual inspection of the trajectories confirmed that none of the ligands exited their respective binding sites during the simulation.

Our electrostatic potential analyses, as depicted in Fig. 1C, reveal a pronounced reconfiguration of charge distributions within the vanilloid pocket upon apocynin ligand binding, in stark contrast to the binding of CAP and CZP. Notably, in the presence of the apocynin ligand, the binding site undergoes a significant shift towards a predominantly electronegative state on its interior, while externally it exhibits a comparatively more electroneutral character than what is observed following the binding of CAP or CZP. This altered electronegativity within the site may offer valuable insights into the RMSD profiles observed for the apocynin ligand.

The comprehensive energetic analysis of the complexes over the entire trajectory (Fig. 1D) unveiled notable differences among them. Specifically, the TRPV1-Apo complex exhibited a comparatively lower level of energetically favorable interactions, whereas the TRPV1-CZP complex displayed the highest favorability. Notably, none of the three complexes demonstrated abrupt changes in their energy profiles

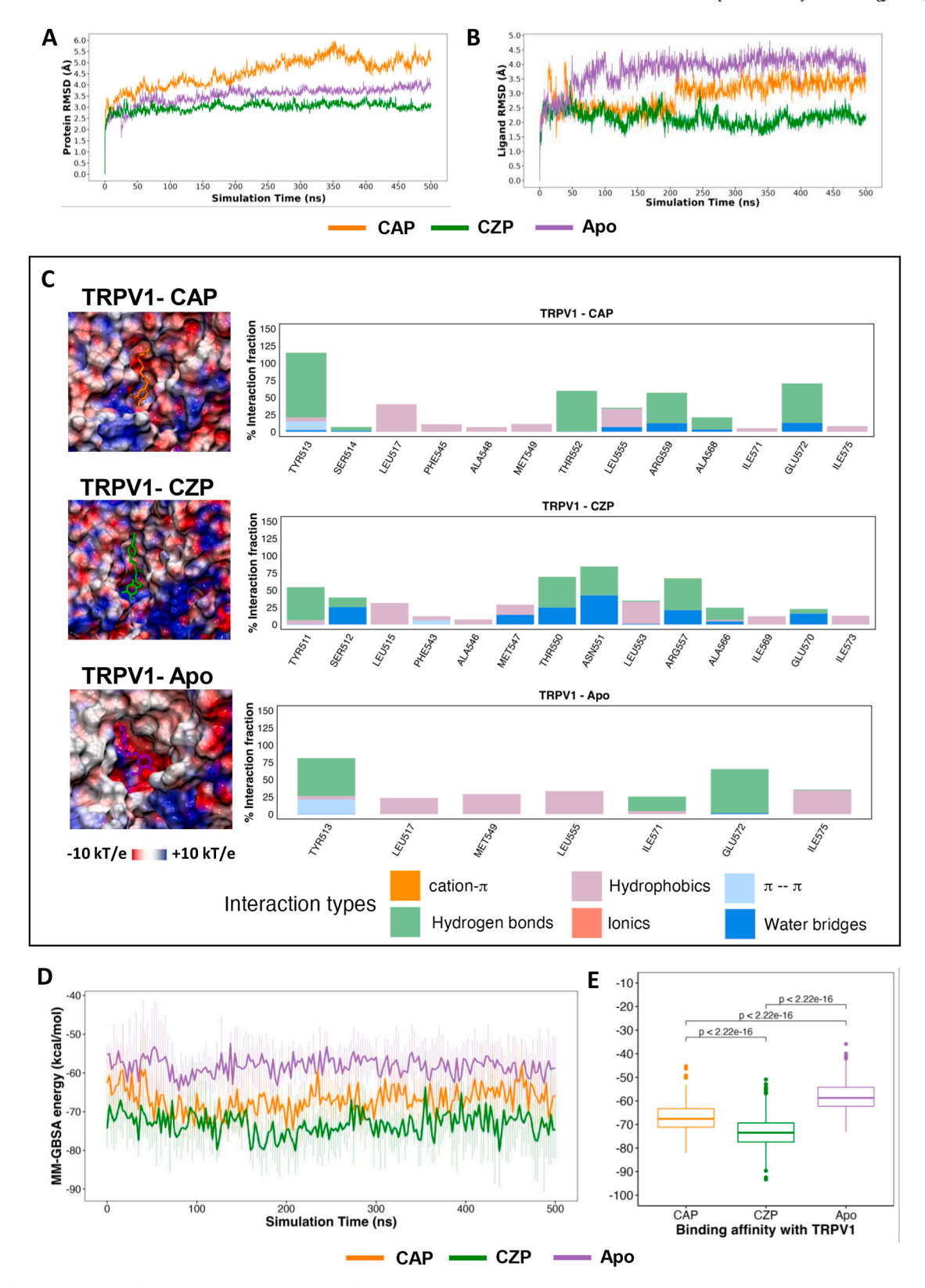


Fig. 1. Stability, Geometric and Energetic profiles for TRPV1-ligand complexes. Root Mean Square Deviation (RMSD) profiles for TRPV1-CAP, TRPV1-CZP, and TRPV1-Apo complexes, depicting the thermodynamic stability of (A) proteins and (B) ligands throughout the 0.5 μs of simulation. Geometric analysis of TRPV1-CAP, TRPV1-CZP, and TRPV1-Apo complexes during the simulation. (C) Electrostatic potential analysis reveals charge redistribution within the vanilloid binding pocket upon ligand binding, represented by the color scheme: red for electronegative, white for electroneutral, and blue for electropositive regions. Intermolecular interactions observed within each complex are illustrated. Energetic analysis of TRPV1-ligand complexes. (D) Illustrates the energy profiles of the TRPV1-CAP, TRPV1-CZP, and TRPV1-Apo complexes, highlighting their respective energetic favorabilities throughout the simulation time. (E) Statistical analysis of a Student's t-test comparing each pair.

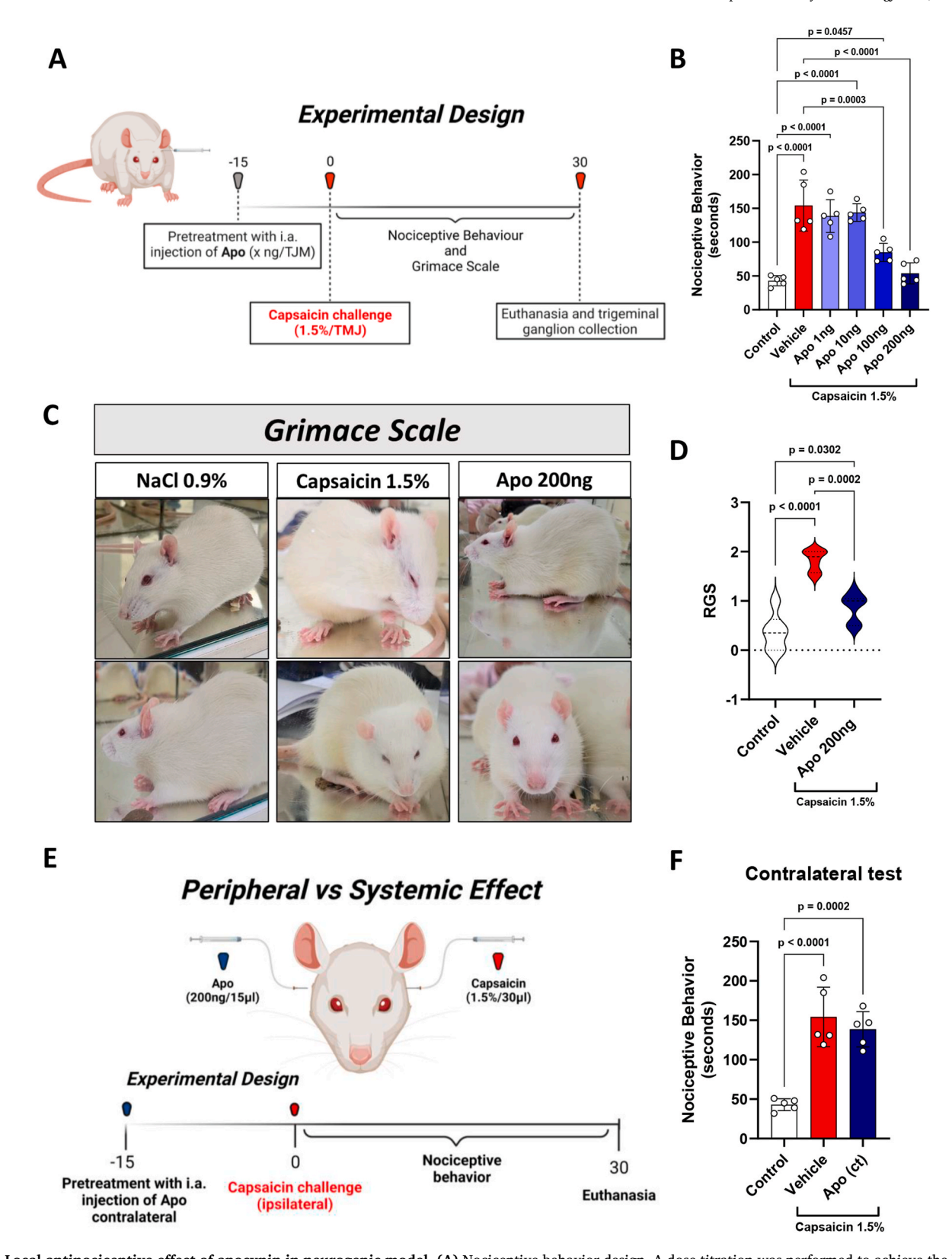


Fig. 2. Local antinociceptive effect of apocynin in neurogenic model. (A) Nociceptive behavior design. A dose titration was performed to achieve the best dose with antinociceptive actions. Capsaicin was used as a noxious agent for the neurogenic model of orofacial pain. The nociceptive score was determined by measuring the number of seconds of rubbing the orofacial region asymmetrically with the ipsilateral fore or hind paw and/or flinching the head in an intermittent and reflexive way characterized by high-frequency shakes of the head. (B) Nociceptive behavior assessment. (C) Representative images from the Grimace Scale. (D) Grimace scale quantification. (E) Contralateral nociceptive behavior design. Animals were pretreated with a contralateral intra-TMJ injection of apocianin (200ng/TMJ) 15 min before the noxious challenge with capsaicin. (F) Nociceptive behavior assessment of the contralateral test. $^*P < 0.05$, $^*P < 0.01$, $^*P < 0.001$, $^*P < 0.001$. $^*P <$

throughout the 0.5 μ s of simulation, indicating the binding site's capacity to maintain ligand stability in a favorable manner over extended periods. A statistical analysis (Fig. 1E) revealed that apocynin exhibits an energy difference of approximately 9 kcal/mol (median energy: -58.71 kcal/mol) compared to CAP (median energy: -67.59 kcal/mol) and a nearly 15 kcal/mol difference relative to CZP (median energy: -73.48) over the course of 200 sampled frames.

Finally, our *in vitro* assay depicts the positive allosteric activity of apocynin on the vanilloid receptor TRPV1. Data showed that the half maximal inhibitory concentration (IC₅₀) for apocynin is 2.3 nM, whereas the antagonist of TRPV1 channel BCTC is 3.6 nM, representing a 1.56-fold reduction (Table 1).

3.2. Intra-TMJ injection of apocynin inhibited capsaicin-induced nociception

Here, we utilize capsaicin as a harmful agent to elicit pain. Initially, we performed a dose-response curve of apocynin administrated locally in the TMJ. For that, different dosages were injected intra-TMJ, followed by capsaicin challenge (Fig. 2). Our results demonstrated that 100 and 200 ng doses per TMJ hinder capsaicin-induced nociception (Fig. 2B). Furthermore, 200 ng per TMJ reversed the nociception and returned it to the homeostatic stages since no differences were observed compared to the control group. In the RGS, where facial expressions were used to assess pain (Fig. 2C), apocynin (200ng/15µl/TMJ) reduced the overall score (Fig. 2D). Lastly, in attempting to clarify whether this effect was exclusively peripheral or if the dosage was high enough to reach systemic circulation, apocynin was injected contralateral from the capsaicin challenge (Fig. 2E). Our findings showed that intra-TMJ injection of apocynin contralaterally did not reverse the capsaicin-induced nociception (Fig. 2F), confirming that the effect of apocynin (200 ng) was strictly peripheral.

3.3. Reduced numbers of $TRPV1^+$ cells post-apocynin treatment in capsaicin-induced nociception

As previously demonstrated, the apocynin molecule showed a great binding affinity with the TRPV1 receptor (Fig. 1). It is known that capsaicin induces pain by stimulating nociceptive neurons through TRPV1 activation and, consequently, depolarization (Wood et al., 1988; Oh et al., 1996). Thus, our immunohistochemistry revealed an increased number of TRPV1⁺ neurons in TG (Fig. 3A), and the apocynin decreased the number of TPRV1⁺ positive cells (Fig. 3B). Representative images are shown in Fig. 3C. 3.4. The impact of apocynin on MAPK activation and neurotransmitter release in TG.

Subsequently, we further investigate the mechanism implicated in the antinociceptive effect of apocynin. Previous literature has demonstrated that TRPV1 and TRPA1 form a complex of channel heteromers and functionally interact in sensory neurons (Spahn et al., 2014), leading to mitogen-activated protein kinase (MAPK) activation and neurotransmitter release (e.g., substance P and CGRP) (Fattori et al., 2016). Initially, as shown in Fig. 4A, we quantified the protein expression of

Table 1 Allosteric activity of apocynin compound on the vanilloid receptor TRPV1. Values were obtained in three independent experiments and expressed average as mean \pm SD (n = 3). Capsaicin was used at 20 nM.

Compound	IC ₅₀ (nM)
Apocynin BCTC	$\begin{array}{c} 2.3\pm1.8\\ 3.6\pm0.51\end{array}$

 ${\rm IC}_{50}$: half maximal inhibitory concentration; BCTC: transient receptor potential vanilloid 1 (TRPV1) antagonist.

TRPV1 (Fig. 4B) and TRPA1 (Fig. 4C) in the TG, and we found that intra-TMJ injection of apocynin significantly increased the expression of TRPA1 but not TRPV1. Furthermore, 1 out of 3 MAPK seems to be involved in capsaicin algic effects (Fig. 4D, E and F). The expression of extracellular signal-regulated kinases (ERKs) (Fig. 4D) was increased by capsaicin and downregulated by intra-TMJ injection of apocynin. At the same time, p38 mitogen-activated protein kinases (p38) and (c-Jun N-terminal kinases) JNK did not change among the groups (Fig. 4E and F). Finally, we quantify the amount of two essential neuropeptides associated with pain signaling (substance P and CGRP) and the neurotransmitter glutamate (Fig. 4G, H, and I) in the whole ganglion. Our results show that intra-TMJ injection of apocynin reduces the higher levels of substance P and CGRP (Fig. 4G and H), while no differences were observed in the levels of glutamate among the groups (Fig. 4I).

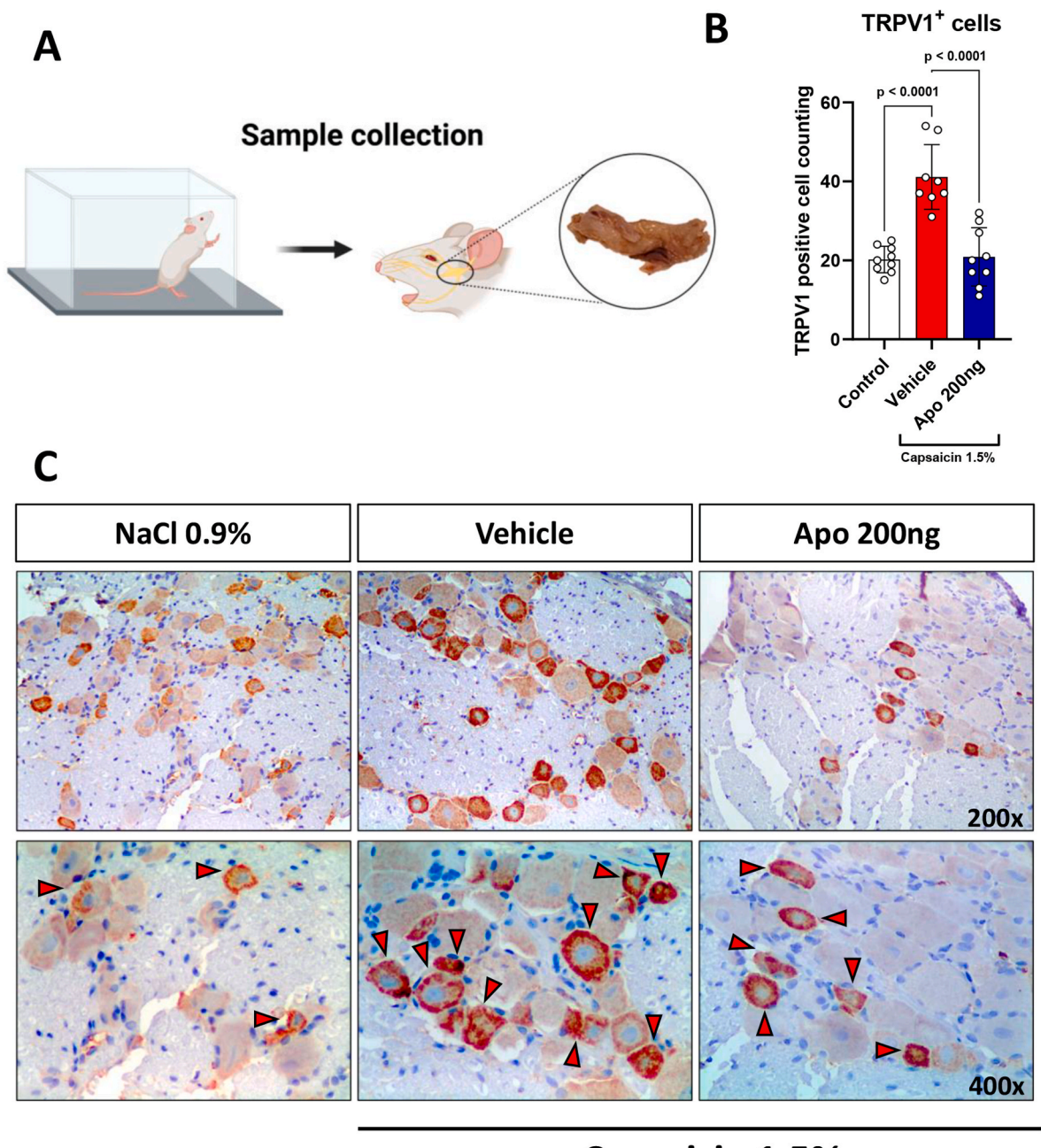
3.4. In vivo toxicity in Galleria mellonella

The toxicity of apocynin was evaluated at different doses using *Galleria mellonella* larvae (Fig. 5A). According to the results (Fig. 5B), it was found that the administration of apocynin at a dose equal to or greater than 600 mg/kg was capable of causing the mortality of 100% of *Galleria mellonella* larvae within 24 h. On the other hand, the administration of apocynin at doses of 0.1 mg/kg to 100 mg/kg did not present toxicity to *Galleria mellonella* larvae in the 24, 48 and 72 h of observation. The median lethal dose (LD50) for apocynin was experimentally determined to be approximately 460 mg/kg. According to the Canadian Centre for Occupational Health and Safety (CCOHS, 2018), the LD50 result classifies apocynin as a slightly toxic compound. This category encompasses values ranging from 350 to 2810 mg/kg.

4. Discussion

The present study applied molecular docking to foretell the more promising chalcone-derived apocynin with greater stability, geometric, and energetic profiles for TRPV1-ligand complexes. In vitro studies using primary cell culture of trigeminal ganglion were carried out to analyze apocynin's capacity to counteract TRPV1 activation by capsaicin. Furthermore, an in vivo model of neurogenic pain elicited by capsaicin was conducted to explore the therapeutic potential of apocynin in orofacial pain in rodents and the mechanism behind its effects. Lastly, in vivo toxicity of apocynin was performed in a survival assay on the Galleria mellonella larvae model. Herein, we demonstrated that apocynin has outstanding pharmacokinetics and binding properties against TRPV1 receptors and ultimately hindered trigeminal neuron activation upon the capsaicin challenge. In vivo, apocynin showed antinociceptive peripheral effects, decreasing the number of immunopositive TRPV1⁺ cells in the trigeminal ganglion, reducing extracellular signal-regulated kinase 1/2 (ERK1/2) phosphorylation, and reducing substance P and CGRP release. In addition, the apocynin demonstrated a slightly toxic compound in the Galleria mellonela model. Overall, we provide proof of principles that apocynin can be elected as a potential pharmacological alternative to manage orofacial pain, particularly those of a neuropathic nature. However, clinical tests must be carried out to prove its effectiveness in orofacial pain.

The results of molecular docking for the apocynin ligand indicate its placement within the vanilloid pocket, a well-known binding site previously characterized for modulators like CAP and CZP. Given the vanilloid-like nature of the apocynin ligand, particularly when compared to the head region of CAP and CZP, it is reasonable to presume its localization within this binding site. Previous research has also indicated that compounds sharing this vanilloid anchoring region tend to occupy this specific site (Bustos et al., 2023). This higher RMSD profile observed for the apocynin ligand within the binding site may be attributed to a potential discrepancy in its initial spatial configuration originating from the molecular docking process. This effect was not observed when utilizing the CAP and CZP conformations obtained from



Capsaicin 1.5%

Fig. 3. TRPV1 protein expression in trigeminal ganglion. (A) Drawing of trigeminal ganglion collection. (B) Counting of immune positive cells for TRPV1 $^+$ in the trigeminal ganglion and (C) representative immunohistochemistry (IHC) images in each group. Magnification:×200 and ×400. 3 independent observers analyzed each slide. Arrowheads indicate immune positive cells for TRPV1 $^+$ in the trigeminal ganglion. White bar represents the control group (intra-TMJ injection of saline solution; NaCl0,9%). ***P < 0.001. Data are expressed as mean \pm SD. n = 3 animals per group in IHC analysis. ANOVA and Tukey's test.

structures derived from Cryo-Electron Microscopy methods. It is crucial to note that the TRPV1 channel complexes employed in this study, specifically TRPV1-CAP and TRPV1-Apo, originate from *Ictidomys tridecemlineatus*, a mammalian species. In contrast, the TRPV1-CZP complex originates from *Rattus norvegicus*. This distinction results in a shift in residue numbering within the vanilloid binding site. Regarding the intermolecular interactions between each ligand and the binding site in TRPV1, we observed that the Apo ligand maintains the same interactions previously reported for the vanilloid head of CAP and CZP. These interactions include hydrogen bonds (HBs) with TYR513 and GLU572 (TYR511 and GLU570 in TRPV1-CZP). Additionally, TYR513 forms π - π interactions with Apo, akin to what was found with CAP. Notably, the

residue ILE571 forms HBs with Apo, in contrast to the interactions observed with the other two ligands. The remaining interactions that anchor Apo within the binding site are predominantly hydrophobic in nature

The discovery that capsaicin could be used as a harmful agent in a pain model was a landmark in the pain and pharmacology field (Wood et al., 1988; Oh et al., 1996). It was also through this discovery that other studies were conducted to comprehend the involvement of TRPV1 receptors in this process (Sluka and Willis, 1997). One of the first pieces of evidence on the mechanism of action of capsaicin revealed that it lowered the thermal threshold in rats and humans (Caterina et al., 1997, 1999, 2000). Furthermore, evidence was presented regarding the

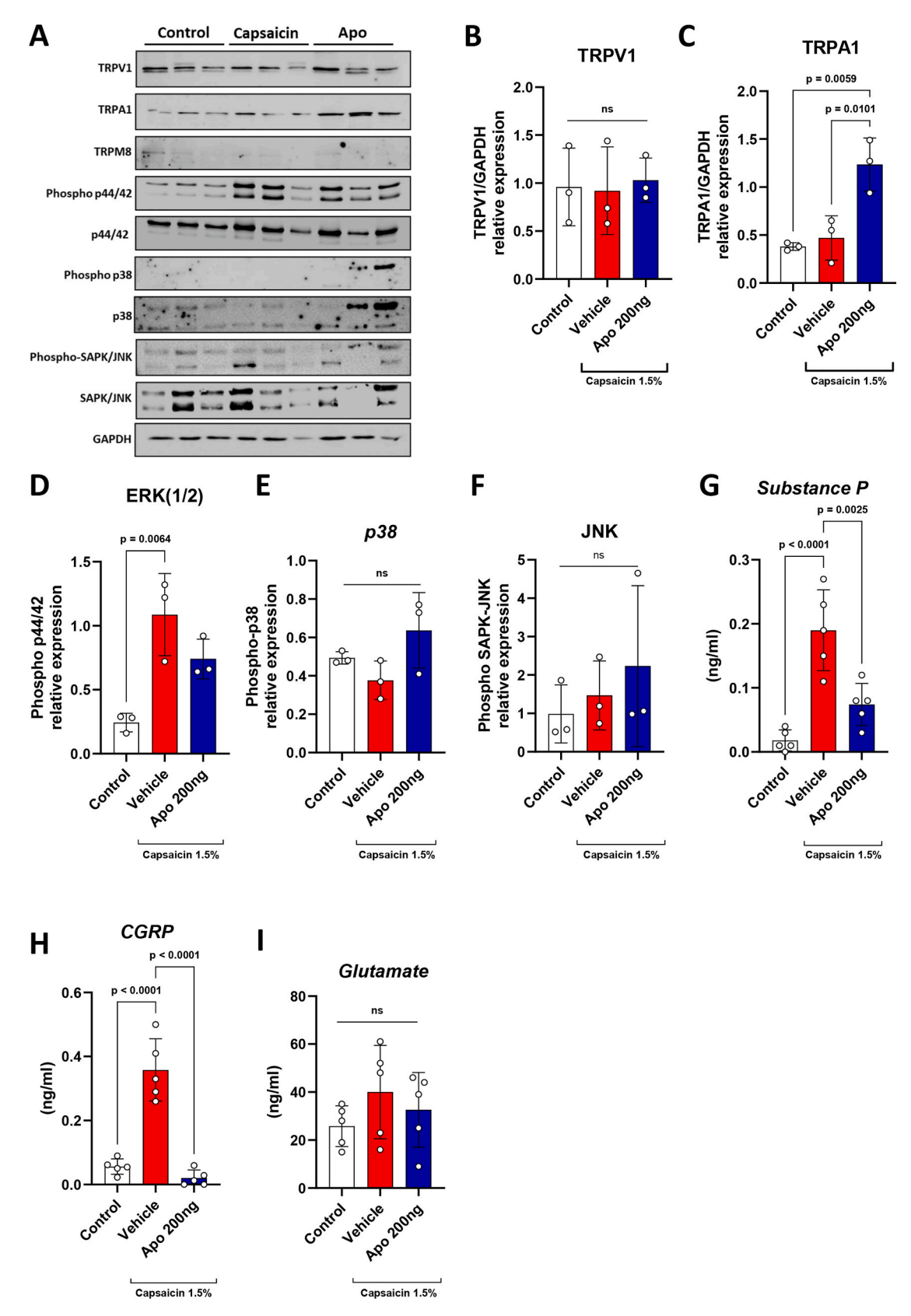


Fig. 4. Apocynin affects TRPA1 and ERK1/2 expression while reducing neuropeptide release in trigeminal ganglion. (A) Representative western blotting images from all targets. Protein levels of (B) TRVP1, (C) TRPA1, (D) ERK1/2, (E) p38, (F) JNK, (G) substance P, (H) CGRP, and (I) glutamate. The protein level of TRPM8 was not included due to absence of protein labeling. *P < 0.05, **P < 0.01, ***P < 0.001, ***P < 0.0001. ns: not significant. White bar represents the control group (intra-TMJ injection of saline solution; NaCl0,9%). The data are expressed as mean \pm S.D.; n = 5 animals per group in ELISA assay; n = 3 animals per group in western Blot analysis. ANOVA and Tukey's test.

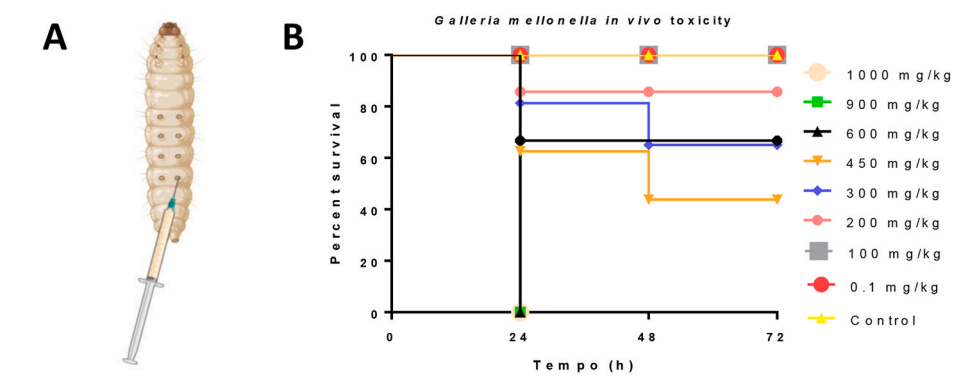


Fig. 5. The effects of apocynin on the systemic toxicity of *Galleria mellonella* larvae. (A) Representative image of the application site. (B) Larvae (n = 15) were treated with apocynin at 0.1, 100, 200, 300, 450, 600, 900 and 1000 mg/kg or mineral water (control) and had their survival monitored over 72 h. Log-rank Mantel—Cox test.

involvement of MAPKs and the neurotransmitter CGRP in this pain process (Sun et al., 2003; Sweitzer et al., 2004). In this sense, we opted for capsaicin as the noxious challenge to investigate the potential analgesic role of apocynin. Herein, we treated the rats with a dose titration of intra-articular injection of apocynin, and we found that the analgesic effect started at a dosage of 100 ng. However, only with 200 ng, the nociceptive score was equivalent to that of the negative control group (intra-articular saline injection). Moreover, we demonstrated that apocynin's antinociceptive effect was exclusively local, which could prevent any side effect or first-pass metabolism that could shrink their therapeutic properties. By way of comparison, tramadol (an opioid used worldwide) induces antinociception ranging from 90 to 500 µg when injected into the temporomandibular joint (Abdalla et al., 2019; Lamana et al., 2017), which is 450 - 2500-fold more heightened, respectively.

TRPV1 is a receptor capable of transducing noxious (thermal) stimulus into nociceptor depolarization, mainly expressed in primary neurons, including TG (Caterina et al., 1997; Tominaga et al., 1998). For instance, mice with genetic deletion of TRPV1 show lower nociceptive reactions against heat and capsaicin challenges (Caterina et al., 2000). Furthermore, in thermal hyperalgesia induced by carrageenan, the disruption of TRPV1 counteracts the inflammatory pain mouse model of dry eye disease, where local inflammation triggers TRPV1, consequently causing corneal nerve damage (Pizzano et al., 2024). Therefore, inhibition of TRPV1 has been tested in distinct pain modalities with promising findings.

Transient receptor potential (TRP) ion channels, including members of the vanilloid TRP (TRPV), melastatin TRP (TRPM), canonical TRP (TRPC), and ankyrin TRP (TRPA) families, have drawn attention for their roles in myriad sensory functions (Fernandes et al., 2012). Both TRPV1 and TRPA1 play a critical role in inflammation and tissue damage and therefore have great potential as drug targets (Liang et al., 2023). We observed that intra-TMJ injection of apocynin significantly increased the expression of TRPA1, but not TRPV1. TRPA1 is widely expressed in neuronal and non-neuronal cells and has been proposed as a nociceptor mediating acute and inflammatory pain (Bautista et al., 2006; Kwan et al., 2006) through studies that demonstrated suppression of sensitivity to mechanical and cold stimuli and induced hyperalgesia in transgenic TRPA1-deficient mice (Obata et al., 2005; Kwan et al., 2006; Karashima et al., 2009). Interestingly, growing evidence has reported that activation of TRPV1 and TRPA1 causes increased intestinal motility and protective effects against gastrointestinal injury via neurotransmitter stimulation (Kojima et al., 2014; Liu et al., 2023). NADPH oxidase (NOX) inhibitors, as such the apocynin family, have been shown to activate TRPA1 in human embryonic kidney cells and human fibroblast-like synoviocytes (Suzuki et al., 2014). Herein, although TRPA1 is associated with painful sensations, including in the trigeminal system (e.g., migraine) (Iannone et al., 2022), we demonstrated that the antinociceptive effects produced by apocynin were not changed, despite

the boost in TRPA1 expression (Fischer et al., 2014). We speculate that: First, neurogenic inflammation is reduced, as shown by the low levels of Substance P and CGRP. Second, when treated with apocynin, the animals do not exhibit nociceptive behavior, supporting the antinociceptive role of apocynin in regulating neurogenic inflammation. Third, the literature indicates that these receptors may interact with each other by forming a TRPV1:TRPA1 heterotetramer. They regulate each other through compensatory and cross-sensitization mechanisms between these two sensory channels (Fischer et al., 2014; Patil et al., 2010; Salas et al., 2009). Therefore, the overexpression of TRPA1, while associated with nociceptive response in some models, does not change the antinociceptive outcome obtained here. Lastly, although there has been increased expression of TRPA1, it does not necessarily mean it is activated (e.g., Ca2+ influx) (Fernandes et al., 2012).

We also found that apocynin-mediated inhibition of TRPV1 decreases the expression of ERKs and reduces the levels of substance P and CGRP. As mentioned previously, TRPV1 activation leads to the release of substance P and CGRP, which are neuropeptides widely distributed in areas of the central and peripheral nervous systems, playing an important role in pain neurotransmission (Fattori et al., 2016). TRPV1 has been shown to co-localize with substance P and CGRP in a dextran sulfate sodium-induced colitis model (Lapointe et al., 2015). Indeed, pharmacological blockage of TRPV1 inhibited capsaicin-induced substance P release in cultured dorsal root ganglion (DRG) neurons (Tang et al., 2008). Additionally, it was reported that Maresin-2 (MaR2), a specialized pro-resolution lipid mediator (SPM), inhibits the activation of TRPV1 and TRPA1, as well as reducing the release of CGRP and decreases pain and inflammation in a model of pain in lipopolysaccharide (LPS)-induced mice (Fattori et al., 2022).

X'Neurogenic inflammation is initiated by the release of neuropeptides such as SP and CGRP, and neurokinin A from sensory nerve endings in response to noxious stimuli (Iannone et al., 2022). These neuropeptides interact with immune cells, endothelial cells, and fibroblasts, leading to vasodilation, increased vascular permeability, and immune cell recruitment, which amplifies the inflammatory response through the release of cytokines and prostaglandins (Koyuncu et al., 2019; Kilinc et al., 2024). Inhibition of the TRPV1 channel can reduce neurogenic inflammation by preventing the activation of sensory neurons that release these pro-inflammatory neuropeptides (Caterina et al., 1999; Caterina and Julius, 2001). TRPV1, which responds to heat, acid, and capsaicin, facilitates the release of neuropeptides that sustain inflammation (Caterina et al., 1999; Caterina and Julius, 2001). By blocking TRPV1, as performed by apocynin, the release of SP and CGRP is limited, ultimately alleviating neurogenic inflammation and associated pain.

In conclusion, we provide proof-of-principles that the newly synthesized apocynin compound effectively prevented nociception in a neurogenic model of orofacial pain. Mechanistically, the treatment with apocynin reduced the number of TRPV1⁺ immunopositive cells,

decreased the release of substance P and CGRP, reduced the phosphorylation of ERK in the trigeminal ganglion, and demonstrated low toxicity.

CRediT authorship contribution statement

Taisa Maria Mendes Matuiama Machado: Writing – original draft, Methodology, Investigation, Data curation. Iara Gonçalves Aquino: Writing – original draft, Methodology, Investigation, Data curation. Marcelo Franchin: Writing – review & editing, Methodology, Investigation, Data curation. Miguel O. Zarraga: Methodology, Investigation, Data curation. Daniel Bustos: Methodology, Data curation. Fernanda Papa Spada: Investigation, Data curation. Marcelo Henrique Napimoga: Writing – review & editing, Resources, Formal analysis. Juliana Trindade Clemente-Napimoga: Writing – review & editing, Resources, Formal analysis. Severino Matias Alencar: Methodology, Investigation, Formal analysis. Bruna Benso: Writing – review & editing, Resources, Methodology, Funding acquisition, Formal analysis, Conceptualization. Henrique Ballassini Abdalla: Writing – review & editing, Writing – original draft, Software, Resources, Methodology, Investigation, Formal analysis, Data curation, Conceptualization.

Data availability statement

The data that support the findings of this study are available from the corresponding author upon reasonable request.

Funding

The authors disclosed receipt of the following financial support for the research, authorship, and/or publication of this article: This work was partially supported by the São Paulo Research Foundation (FAPESP, 2017/22334-9) to M.H.N. and by the ANID/Fondecyt Iniciacion (#11230490) to B.B.

Declaration of competing interest

All authors declare that they have no competing interests.

Acknowledgments

The authors thank Nadir de Freitas and Elisangela for histological technical assistance and animal care, respectively.

Appendix A. Supplementary data

Supplementary data to this article can be found online at https://doi.org/10.1016/j.ejphar.2024.177093.

Data availability

Data will be made available on request.

References

- Abdalla, H.B., Jain, A.K., Napimoga, M.H., Clemente-Napimoga, J.T., Gill, H.S., 2019. Microneedles coated with tramadol exhibit antinociceptive effect in a rat model of temporomandibular hypernociception. J Pharmacol Exp Ther 370 (3), 834–842. https://doi.org/10.1124/jnet.119.256750.
- Abdalla, H.B., Napimoga, M.H., de Macedo Maganin, A.G., Lopes, A.H., Cunha, T.M., Gill, H.S., Clemente-Napimoga, J.T., 2021. The role of adenosine A1 receptor in the peripheral tramadol's effect in the temporomandibular joint of rats. Int Immunopharmacol 97. 107680. https://doi.org/10.1016/j.intimp.2021.107680.
- Abdalla, H.B., Napimoga, M.H., Teixeira, J.M., Trindade-da-Silva, C.A., Pieroni, V.L., Dos Santos Araújo, F.S.M., Hammock, B.D., Clemente-Napimoga, J.T., 2022a. Soluble epoxide hydrolase inhibition avoid formalin-induced inflammatory hyperalgesia in the temporomandibular joint. Inflammopharmacology 30 (3), 981–990. https://doi. org/10.1007/s10787-022-00965-5.

- Abdalla, H.B., Napimoga, M.H., Trindade-da-Silva, C.A., Guimarães, M., Lopes, M., Dos Santos, P.C.V., Buarque, E., Silva, W.A., Andrade, E., Silva, F., Clemente-Napimoga, J.T., 2022b. Occlusal trauma induces neuroimmune crosstalk for a pain state. J. Dent. Res. 101 (3), 339–347. https://doi.org/10.1177/00220345211030482
- Baker, N.A., Sept, D., Joseph, S., Holst, M.J., McCammon, J.A., 2001. Electrostatics of nanosystems: application to microtubules and the ribosome. Proc. Natl. Acad. Sci. U. S. A. 98 (18), 10037–10041. https://doi.org/10.1073/pnas.181342398.
- Bautista, D.M., Jordt, S.E., Nikai, T., Tsuruda, P.R., Read, A.J., Poblete, J., Yamoah, E.N., Basbaum, A.I., Julius, D., 2006. TRPA1 mediates the inflammatory actions of environmental irritants and proalgesic agents. Cell 124 (6), 1269–1282. https://doi. org/10.1016/j.cell.2006.02.023.
- Benso, B., Bustos, D., Zarraga, M.O., Gonzalez, W., Caballero, J., Brauchi, S., 2019. Chalcone derivatives as non-canonical ligands of TRPV1. Int. J. Biochem. Cell Biol. 112, 18–23. https://doi.org/10.1016/ji.biocel.2019.04.010.
- Biscetti, L., Cresta, E., Cupini, L.M., Calabresi, P., Sarchielli, P., 2023. The putative role of neuroinflammation in the complex pathophysiology of migraine: from bench to bedside. Neurobiol. Dis. 180, 106072. https://doi.org/10.1016/j.nbd.2023.106072.
- Bustos, D., Galarza, C., Ordoñez, W., Brauchi, S., Benso, B., 2023. Cost-effective pipeline for a rational design and selection of capsaicin analogues targeting TRPV1 channels. ACS Omega 8 (13), 11736–11749. https://doi.org/10.1021/acsomega.2c05672.
- Caterina, M.J., Julius, D., 2001. The vanilloid receptor: a molecular gateway to the pain pathway. Annu. Rev. Neurosci. 24, 487–517. https://doi.org/10.1146/annurev. neuro.24.1.487.
- Caterina, M.J., Schumacher, M.A., Tominaga, M., Rosen, T.A., Levine, J.D., Julius, D., 1997. The capsaicin receptor: a heat-activated ion channel in the pain pathway. Nature 389 (6653), 816–824. https://doi.org/10.1038/39807.
- Caterina, M.J., Rosen, T.A., Tominaga, M., Brake, A.J., Julius, D., 1999. A capsaicin-receptor homologue with a high threshold for noxious heat. Nature 398 (6726), 436–441. https://doi.org/10.1038/18906.
- Caterina, M.J., Leffler, A., Malmberg, A.B., Martin, W.J., Trafton, J., Petersen-Zeitz, K.R., Koltzenburg, M., Basbaum, A.I., Julius, D., 2000. Impaired nociception and pain sensation in mice lacking the capsaicin receptor. Science 288 (5464), 306–313. https://doi.org/10.1126/science.288.5464.306.
- Davis, J.B., Gray, J., Gunthorpe, M.J., Hatcher, J.P., Davey, P.T., Overend, P., Harries, M. H., Latcham, J., Clapham, C., Atkinson, K., Hughes, S.A., Rance, K., Grau, E., Harper, A.J., Pugh, P.L., Rogers, D.C., Bingham, S., Randall, A., Sheardown, S.A., 2000. Vanilloid receptor-1 is essential for inflammatory thermal hyperalgesia. Nature 405 (6783), 183–187. https://doi.org/10.1038/35012076.
- Ettlin, D.A., Napimoga, M.H., Meira, E., Cruz, M., Clemente-Napimoga, J.T., 2021. Orofacial musculoskeletal pain: an evidence-based bio-psycho-social matrix model. Neurosci. Biobehav. Rev. 128, 12–20. https://doi.org/10.1016/j. neubjorev.2021.06.008.
- Fattori, V., Hohmann, M.S., Rossaneis, A.C., Pinho-Ribeiro, F.A., Verri, W.A., 2016. Capsaicin: current understanding of its mechanisms and therapy of pain and other pre-clinical and clinical uses. Molecules 21 (7), 844. https://doi.org/10.3390/ molecules21070844.
- Fattori, V., Zaninelli, T.H., Ferraz, C.R., Brasil-Silva, L., Borghi, S.M., Cunha, J.M., Chichorro, J.G., Casagrande, R., Verri Jr., W.A., 2022. Maresin 2 is an analgesic specialized pro-resolution lipid mediator in mice by inhibiting neutrophil and monocyte recruitment, nociceptor neuron TRPV1 and TRPA1 activation, and CGRP release. Neuropharmacology 216, 109189. https://doi.org/10.1016/j. neuropharm.2022.109189.
- Fernandes, E.S., Fernandes, M.A., Keeble, J.E., 2012. The functions of TRPA1 and TRPV1: moving away from sensory nerves. Br. J. Pharmacol. 166 (2), 510–521. https://doi.org/10.1111/j.1476-5381.2012.01851.x.
- Fischer, M.J., Balasuriya, D., Jeggle, P., Goetze, T.A., McNaughton, P.A., Reeh, P.W., Edwardson, J.M., 2014. Direct evidence for functional TRPV1/TRPA1 heteromers. Pflügers Archiv 466 (12), 2229–2241. https://doi.org/10.1007/s00424-014-1497-z. Fpub 2014 Mar 19.
- Gao, Y., Cao, E., Julius, D., Cheng, Y., 2016. TRPV1 structures in nanodiscs reveal mechanisms of ligand and lipid action. Nature 534 (7607), 347–351. https://doi. org/10.1038/nature17964.
- Ghurye, S., McMillan, R., 2017. Orofacial pain an update on diagnosis and management. Br. Dent. J. 223 (9), 639–647. https://doi.org/10.1038/sj. bdi.2017.879.
- Grant, B.J., Skjaerven, L., Yao, X.Q., 2021. The Bio3D packages for structural bioinformatics. Protein Sci. 30 (1), 20–30. https://doi.org/10.1002/pro.3923
- Halgren, T.A., Murphy, R.B., Friesner, R.A., Beard, H.S., Frye, L.L., Pollard, W.T., Banks, J.L., 2004. Glide: a new approach for rapid, accurate docking and scoring. 2. Enrichment factors in database screening. J. Med. Chem. 47 (7), 1750–1759. https://doi.org/10.1021/jm030644s.
- Harper, D.E., Schrepf, A., Clauw, D.J., 2016. Pain mechanisms and centralized pain in temporomandibular disorders. J. Dent. Res. 95 (10), 1102–1108. https://doi.org/ 10.1177/0022034516657070.
- Humphrey, W., Dalke, A., Schulten, K., 1996. VMD: visual molecular dynamics. J. Mol. Graph. 14 (1), 33–38. https://doi.org/10.1016/0263-7855(96)00018-5, 27-38.
- Iannone, L.F., De Logu, F., Geppetti, P., De Cesaris, F., 2022. The role of TRP ion channels in migraine and headache. Neurosci. Lett. 768, 136380. https://doi.org/10.1016/j. neulet.2021.136380.
- International Classification of Orofacial Pain, 2020. In: (ICOP). Cephalalgia, first ed., vol. 40, pp. 129–221. https://doi.org/10.1177/0333102419893823 2.
- Jacobson, M.P., Pincus, D.L., Rapp, C.S., Day, T.J., Honig, B., Shaw, D.E., Friesner, R.A., 2004. A hierarchical approach to all-atom protein loop prediction. Proteins 55 (2), 351–367. https://doi.org/10.1002/prot.10613.

- Karashima, Y., Talavera, K., Everaerts, W., Janssens, A., Kwan, K.Y., Vennekens, R., Nilius, B., Voets, T., 2009. TRPA1 acts as a cold sensor in vitro and in vivo. Proc. Natl. Acad. Sci. U. S. A. 106 (4), 1273–1278. https://doi.org/10.1073/ pngs.0808487106
- Kilinc, E., Torun, I.E., Baranoglu Kilinc, Y., 2024. Meningeal mast cell-mediated mechanisms of cholinergic system modulation in neurogenic inflammation underlying the pathophysiology of migraine. Eur. J. Neurosci. 59 (9), 2181–2192. https://doi.org/10.1111/ejn.15888.
- Kilkenny, C., Browne, W.J., Cuthill, I.C., Emerson, M., Altman, D.G., 2010. Improving bioscience research reporting: the ARRIVE guidelines for reporting animal research. PLoS Biol. 29:8 (6), e1000412.
- Klees, R.F., De Marco, P.C., Salasznyk, R.M., Ahuja, D., Hogg, M., Antoniotti, S., Kamath, L., Dordick, J.S., Plopper, G.E., 2006. Apocynin derivatives interrupt intracellular signaling resulting in decreased migration in breast cancer cells. J. Biomed. Biotechnol. 2006 (2), 87246. https://doi.org/10.1155/JBB/2006/872
- Kojima, R., Nozawa, K., Doihara, H., Keto, Y., Kaku, H., Yokoyama, T., Itou, H., 2014. Effects of novel TRPA1 receptor agonist ASP7663 in models of drug-induced constipation and visceral pain. Eur. J. Pharmacol. 723, 288–293. https://doi.org/ 10.1016/j.eiphar.2013.11.020.
- Koyuncu Irmak, D., Kilinc, E., Tore, F., 2019. Shared fate of meningeal mast cells and sensory neurons in migraine. Front. Cell. Neurosci. 13, 136. https://doi.org/ 10.3389/fncel.2019.00136.
- Kwan, K.Y., Allchorne, A.J., Vollrath, M.A., Christensen, A.P., Zhang, D.S., Woolf, C.J., Corey, D.P., 2006. TRPA1 contributes to cold, mechanical, and chemical nociception but is not essential for hair-cell transduction. Neuron 50 (2), 277–289. https://doi. org/10.1016/j.neuron.2006.03.042.
- Lam, D.K., Sessle, B.J., Cairns, B.E., Hu, J.W., 2005. Peripheral NMDA receptor modulation of jaw muscle electromyographic activity induced by capsaicin injection into the temporomandibular joint of rats. Brain Res. 1046 (1–2), 68–76. https://doi. org/10.1016/j.brainres.2005.03.040.
- Lamana, S.M.S., Napimoga, M.H., Nascimento, A.P.C., Freitas, F.F., de Araujo, D.R., Quinteiro, M.S., Macedo, C.G., Fogaça, C.L., Clemente-Napimoga, J.T., 2017. The anti-inflammatory effect of tramadol in the temporomandibular joint of rats. Eur. J. Pharmacol. 807, 82–90. https://doi.org/10.1016/j.ejphar.2017.04.012.
- Lapointe, T.K., Basso, L., Iftinca, M.C., Flynn, R., Chapman, K., Dietrich, G., Vergnolle, N., Altier, C., 2015. TRPV1 sensitization mediates postinflammatory visceral pain following acute colitis. Am. J. Physiol. Gastrointest. Liver Physiol. 309 (2), G87–G99. https://doi.org/10.1152/ajpgi.00421.2014.
- Liang, Q., Wang, J.W., Bai, Y.R., Li, R.L., Wu, C.J., Peng, W., 2023. Targeting TRPV1 and TRPA1: a feasible strategy for natural herbal medicines to combat postoperative ileus. Pharmacol. Res. 196, 106923. https://doi.org/10.1016/j.phrs.2023.106923.
- Liu, J., Jia, S., Huang, F., He, H., Fan, W., 2022. Peripheral role of glutamate in orofacial pain. Front. Neurosci. 16, 929136. https://doi.org/10.3389/fnins.2022.929136.
- Liu, L., Xu, M., Zhang, Z., Qiao, Z., Tang, Z., Wan, F., Lan, L., 2023. TRPA1 protects mice from pathogenic Citrobacter rodentium infection via maintaining the colonic epithelial barrier function. Faseb. J. 37 (2), e22739. https://doi.org/10.1096/ fj.202200483RRR.
- Luo, J., Zhu, Y., Zhu, M.X., Hu, H., 2011. Cell-based calcium assay for medium to high throughput screening of TRP channel functions using FlexStation 3. J. Vis. Exp. 17 (54), 3149. https://doi.org/10.3791/3149.
- Maestro, S., 2020. Schrödinger Release 2021-1. LLC, New York, NY.
- Mazuqueli Pereira, E.S.B., Basting, R.T., Abdalla, H.B., Garcez, A.S., Napimoga, M.H., Clemente-Napimoga, J.T., 2021. Photobiomodulation inhibits inflammation in the temporomandibular joint of rats. J. Photochem. Photobiol., B 222, 112281. https://doi.org/10.1016/j.jphotobiol.2021.112281.
- Mecklenburg, J., Shein, S.A., Malmir, M., Hovhannisyan, A.H., Weldon, K., Zou, Y., Lai, Z., Jin, Y.F., Ruparel, S., Tumanov, A.V., Akopian, A.N., 2023. Transcriptional profiles of non-neuronal and immune cells in mouse trigeminal ganglia. Front Pain Res (Lausanne) 4, 1274811. https://doi.org/10.3389/fpain.2023.1274811.
- Megaw, J., Thompson, T.P., Lafferty, R.A., Gilmore, B.F., 2015. Galleria mellonella as a novel in vivo model for assessment of the toxicity of 1-alkyl-3-methylimidazolium chloride ionic liquids. Chemosphere 139, 197–201. https://doi.org/10.1016/j. chemosphere.2015.06.026.
- Moreno, Y., 2020. Synthesis and crystal structure analysis of a new chalcone derivative of apocynin. J. Chil. Chem. Soc. 65 (3), 4934–4936.
- Nadezhdin, K.D., Neuberger, A., Nikolaev, Y.A., Murphy, L.A., Gracheva, E.O., Bagriantsev, S.N., Sobolevsky, A.I., 2021. Extracellular cap domain is an essential component of the TRPV1 gating mechanism. Nat. Commun. 12 (1), 2154. https://doi.org/10.1038/s41467-021-22507-3.
- Obata, K., Katsura, H., Mizushima, T., Yamanaka, H., Kobayashi, K., Dai, Y., Fukuoka, T., Tokunaga, A., Tominaga, M., Noguchi, K., 2005. TRPA1 induced in sensory neurons contributes to cold hyperalgesia after inflammation and nerve injury. J. Clin. Invest. 115 (9), 2393–2401. https://doi.org/10.1172/JCI25437.

- Oh, U., Hwang, S.W., Kim, D., 1996. Capsaicin activates a nonselective cation channel in cultured neonatal rat dorsal root ganglion neurons. J. Neurosci. 16 (5), 1659–1667. https://doi.org/10.1523/JNEUROSCI.16-05-01659.1996.
- Olsson, M.H., Søndergaard, C.R., Rostkowski, M., Jensen, J.H., 2011. PROPKA3: consistent treatment of internal and surface residues in empirical pKa predictions. J. Chem. Theor. Comput. 7 (2), 525–537. https://doi.org/10.1021/ct100578z.
- Patil, M.J., Jeske, N.A., Akopian, A.N., 2010. Transient receptor potential V1 regulates activation and modulation of transient receptor potential A1 by Ca2+. Neuroscience 171 (4), 1109–1119. https://doi.org/10.1016/j.neuroscience.2010.09.031.
- Pelissier, T., Pajot, J., Dallel, R., 2002. The orofacial capsaicin test in rats: effects of different capsaicin concentrations and morphine. Pain 96 (1–2), 81–87. https://doi. org/10.1016/s0304-3959(01)00432-8.
- Pizzano, M., Vereertbrugghen, A., Cernutto, A., Sabbione, F., Keitelman, I.A., Shiromizu, C.M., Aguilar, D.V., Fuentes, F., Giordano, M.N., Trevani, A.S., Galletti, J. G., 2024. TRPV1 channels facilitate axonal degeneration of corneal sensory nerves in dry eye. Am. J. Pathol. 5 (24), S0002–S9440. https://doi.org/10.1016/j. aipath.2024.01.015. 00047-6.
- Rocha-Neto, L.M., Gamarra-Suárez, J.R., Freitas, F.F., Muzilli Jr., A., Abdalla, H.B., Macedo, C.G., Napimoga, M.H., Clemente-Napimoga, J.T., 2019. Early phase of type 1 diabetes decreases the responsiveness of C-fiber nociceptors in the temporomandibular joint of rats. Neuroscience 416, 229–238. https://doi.org/ 10.1016/j.neuroscience.2019.08.011.
- Rochelle, S.L.A., Sardi, J.D.C.O., Freires, I.A., de Carvalho Galvão, L.C., Lazarini, J.G., de Alencar, S.M., Rosalen, P.L., 2016. The anti-biofilm potential of commonly discarded agro-industrial residues against opportunistic pathogens. Ind. Crop. Prod. 87, 150–160. https://doi.org/10.1016/j.indcrop.2016.03.044.
- Roos, K., Wu, C., Damm, W., Reboul, M., Stevenson, J.M., Lu, C., Dahlgren, M.K., Mondal, S., Chen, W., Wang, L., Abel, R., Friesner, R.A., Harder, E.D., 2019. OPLS3e: Extending Force Field Coverage for Drug-Like Small Molecules. J. Chem. Theor. Comput. 15 (3), 1863–1874. https://doi.org/10.1021/acs.jctc.8b01026.
- Salas, M.M., Hargreaves, K.M., Akopian, A.N., 2009. TRPA1-mediated responses in trigeminal sensory neurons: interaction between TRPA1 and TRPV1. Eur. J. Neurosci. 29 (8), 1568–1578. https://doi.org/10.1111/j.1460-9568.2009.06702
- Shelley, J.C., Cholleti, A., Frye, L.L., Greenwood, J.R., Timlin, M.R., Uchimaya, M., 2007.
 Epik: a software program for pK(a) prediction and protonation state generation for drug-like molecules. J. Comput. Aided Mol. Des. 21 (12), 681–691. https://doi.org/10.1007/s10822-007-9133-z.
- Sluka, K.A., Willis, W.D., 1997. The effects of G-protein and protein kinase inhibitors on the behavioral responses of rats to intradermal injection of capsaicin. Pain 71 (2), 165–178. https://doi.org/10.1016/s0304-3959(97)03371-x.
- Sotocinal, S.G., Sorge, R.E., Zaloum, A., Tuttle, A.H., Martin, L.J., Wieskopf, J.S., Mapplebeck, J.C., Wei, P., Zhan, S., Zhang, S., McDougall, J.J., King, O.D., Mogil, J. S., 2011. The Rat Grimace Scale: a partially automated method for quantifying pain in the laboratory rat via facial expressions. Mol. Pain 7, 55. https://doi.org/10.1186/1744-8069-7-55.
- Spahn, V., Stein, C., Zöllner, C., 2014. Modulation of transient receptor vanilloid 1 activity by transient receptor potential ankyrin 1. Mol. Pharmacol. 85 (2), 335–344. https://doi.org/10.1124/mol.113.088997.
- Sun, R.Q., Lawand, N.B., Willis, W.D., 2003. The role of calcitonin gene-related peptide (CGRP) in the generation and maintenance of mechanical allodynia and hyperalgesia in rats after intradermal injection of capsaicin. Pain 104 (1–2), 201–208. https://doi. org/10.1016/s0304-3959(03)00008-3.
- Suzuki, H., Hatano, N., Muraki, Y., Itoh, Y., Kimura, S., Hayashi, H., Onozaki, K., Ohi, Y., Haji, A., Muraki, K., 2014. The NADPH oxidase inhibitor diphenyleneiodonium activates the human TRPA1 nociceptor. Am. J. Physiol. Cell Physiol. 307 (4), C384–C394. https://doi.org/10.1152/ajpcell.00182.2013.
- Sweitzer, S.M., Peters, M.C., Ma, J.Y., Kerr, I., Mangadu, R., Chakravarty, S., Dugar, S., Medicherla, S., Protter, A.A., Yeomans, D.C., 2004. Peripheral and central p38 MAPK mediates capsaicin-induced hyperalgesia. Pain 111 (3), 278–285. https://doi.org/10.1016/j.pain.2004.07.007.
- Tang, H.B., Li, Y.S., Miyano, K., Nakata, Y., 2008. Phosphorylation of TRPV1 by neurokinin-1 receptor agonist exaggerates the capsaicin-mediated substance P release from cultured rat dorsal root ganglion neurons. Neuropharmacology 55 (8), 1405–1411. https://doi.org/10.1016/j.neuropharm.2008.08.037.
- Tominaga, M., Caterina, M.J., Malmberg, A.B., Rosen, T.A., Gilbert, H., Skinner, K., Raumann, B.E., Basbaum, A.I., Julius, D., 1998. The cloned capsaicin receptor integrates multiple pain-producing stimuli. Neuron 21 (3), 531–543. https://doi. org/10.1016/s0896-6273(00)80564-4.
- Wood, J.N., Winter, J., James, I.F., Rang, H.P., Yeats, J., Bevan, S., 1988. Capsaicin-induced ion fluxes in dorsal root ganglion cells in culture. J. Neurosci. 8 (9), 3208–3220. https://doi.org/10.1523/JNEUROSCI.08-09-03208.1988.